Tropospheric Ozone Lidar for OMI validation

A.M. Hoexum[1], A. Apituley[1], M.A.F. Allaart[2], A.J.M. Piters[2]

[1]RIVM, P.O. Box 1, 3720 BA Bilthoven, The Netherlands, Mink.Hoexum@RIVM.nl
[2]KNMI, P.O. Box 201, 3730 AE De Bilt, The Netherlands

ABSTRACT

A Differential Absorption Lidar (DIAL) "tropO3" for routine profiling of tropospheric ozone is presented. The instrument is located at RIVM in Bilthoven, The Netherlands (52°07'N, 05°12'E). The instrument was built for routine observations and validation purposes. Within the scope of this project, its measurements will be used in a study to validate tropospheric ozone products from AURA/OMI (Ozone Monitoring Instrument) and to analyse the temporal and spatial variability and representativeness.

The instrument operates at wavelengths within the Hartley band and is therefore suitable for both daytime and nighttime operation. Under clear sky conditions, a full ozone profile from 1 km up to 12 km can be created within one hour, which enables high-resolution time series of tropospheric ozone profiles needed for the variability and representativeness study. Operation under low level cloud conditions with coverage up to 4 octa is possible.

A description of the modernisation of the system is given and a brief re-assessment of the instrument performance is shown. Data is presented from an intensive observation period (CINDI) that will be used in the analysis of satellite data.

1. INTRODUCTION

Tropospheric ozone is a trace gas with key roles in atmospheric chemistry and climate change. Accurate knowledge about the global distribution, variability and trends are required in studies of these topics. Global coverage can only be achieved by observations from space. Unfortunately, tropospheric ozone is difficult to measure by passive spaceborne instruments and a pressing need for quality assessment of new spaceborne platforms exists. High resolution data in time and space is required to adequately study the validity and representativeness of the satellites. The traditional ozone sondes lack the required temporal resolution, but lidar measurements are capable of providing such data. This paper describes tropoO3, built and operated at RIVM, and discusses a dataset for use in the analysis of satellite data.

The instrument was made operational in the 1990's [1] and remained in operation from 1993 to 2003 [2],[3],[4]. A historic data set from this period is available, of which an example is shown in section 4.

Recently, the hardware and software of the instrument were modernised within the framework of a project aimed at strengthening the satellite validation potential of CESAR (Cabauw Experimental Site for Atmospheric Research), which is one of the specific goals of CESAR. The current instrumentation at CESAR features ground-based in-situ and column integrated measurement equipment for tropospheric gases.

2. DESCRIPTION OF THE INSTRUMENT

The DIAL system is based on two frequency-quadrupled Nd:YAG lasers, emitting 266 nm laser light. To create the "on" wavelength, one laser pumps a Raman cell containing a mixture of D_2 and Ar, optimised for first D_2 Stokes emission at 289 nm. The other laser produces the "off" wavelength by pumping a second cell with H_2 and Ar and optimised for first H_2 Stokes emission at 299 nm. The laser light is directed into the atmosphere by means of two steerable mirrors, positioned symmetrically with respect to the telescope.

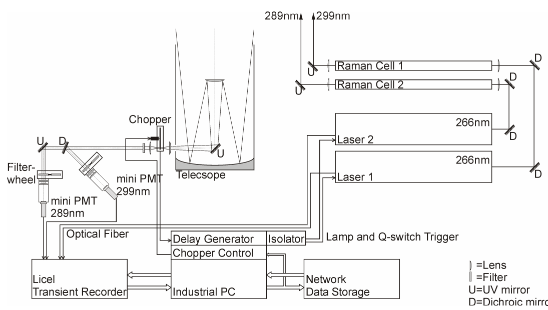

Figure 1, Schematic description of the instrument.

The backscattered light is received by a 60 cm Dall-Kirkham telescope and focused on a mechanical chopper. After passing the chopper, the beam is collimated to a diameter of approximately 25 mm. A dichroic mirror then separates the "on" and "off" signals. Both signals pass their respective narrowband interference filters and filterwheels with ND filters before irradiating mini-PMT's.

The mechanical chopper serves as a master oscillator for the instrument by triggering the flash lamps and Q-switches of both lasers. The emitted laser light subsequently triggers a Licel digitiser, that simultaneously records analog and photon counting data from the mini-PMT's. An industrial PC controls the setup, displays and stores data.

Because of the large dynamic range of the return signal, caused by high atmospheric attenuation at the UV wavelengths, the detectors suffer from memory effects. As a consequence, a full ozone profile can not be created using one instrument setting. Depending on the atmospheric conditions, two or three sequential

© Proceedings of the 8th International Symposium on Tropospheric Profiling, ISBN 978-90-6960-233-2
Delft, The Netherlands, October 2009. Editors, A. Apituley, H.W.J. Russchenberg, W.A.A. Monna

measurements are combined into one ozone profile. The settings distinguish between the *near*, *mid* and *far* range.

3. MODERNISATION OF THE INSTRUMENT

The recent modernisations are aimed at instrument improvement and further automation. Hardware modernisations include the installation of new lasers, detectors, optical filters and filter wheels.

The data processing software was revised, making the conversion from raw data to quicklooks and ozone profiles easier and quicker. Semi-automated removal of clouds from a measurement is amongst the implemented features (Figure 5). Quicklooks from this instrument can be publicly accessed at http://cerberus.rivm.nl/lidar/Bilthoven/TropO3/

3.1 System hardware modernisation

The new lasers, type Spectron SL852, with a table-top beam profile and operating at 30 Hz replaced the Quanta-Ray DCR-3 lasers, which had a doughnut beam profile and operated at 10 Hz. The increased repetition rate and average power should enable measurements under a wider range of atmospheric conditions [5].

Because of the changes in beam profile, intensity distributions in the Raman conversion were altered. Experiments were performed to tune the conversion by optimising the mixtures and pressures in both Raman cells, aiming at the best first Stokes conversion in combination with beam quality. Results are depicted in Figure 2. For this system, the optima were located at 32.5 bar D_2 with 2.5 bar Ar and at 22.5 bar H_2 with 10 bar Ar.

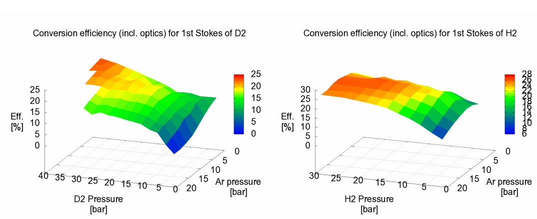

Figure 2, Conversion efficiency graphs for the 1st Stokes of 266 nm in a D_2/Ar mixture (289 nm) and a H_2/Ar mixture (299 nm).

The photomultiplier tubes, Thorn-EMI 9817QA, were replaced by Hamamatsu R7400P mini-PMT's, which were selected for linearity, high gain and suitability for use in photon counting mode. This modification should improve the signal to noise ratio, memory effects and minimum pulse width, thus increasing the maximum measurement range. Each mini-PMT is enclosed in a light-tight housing, fitted with a focusing lens, a filter wheel with ND filters and an interference filter. The use of a filter wheel allows remote control of the return signal strength and the dynamic range.

The old interference filters were replaced by new ones with better out-of-band blocking and smaller bandwidth. The transmissions of the new filters are lower than before (Tab.1), however, a previously installed 289-290 nm bandpass filter can now be eliminated. The relatively low transmission of the 289 nm filter decreased the total transmission at this wavelength, but the increased blocking and smaller bandwidth, caused an improvement in overall performance.

	Old	New
Emitter		
Laser	Quanta-Ray DCR-3	Spectron SL852
Beam profile	Doughnut	table top
Repetition rate (Hz)	10	30
Pulse energy at 266 (mJ)	80	67
Receiver		
Detectors	Thorn-EMI 9817QA	Hamamatsu R7400P
Optical filters	Barr Associates	Barr Associates
Wavelength	289 / 299	289 / 299
Bandwidth (nm)	3	1
Out-of-band blocking	$>10^3$ / $>1.5{\cdot}10^3$	$>10^5$ / $>10^6$
Transmission at 289 and 299 (%)	43 / 60	16 / 29
Total transmission at 289 and 299 (%)	11 / 16	4.8 / 24
Digitiser	LeCroy TR6810	Licel TR20-160
Frequency (MHz/bits)	5/12 bit	20/12 bit
Photon counting ability	–	250 MHz
System control	HP1000 RTE-A	industrial PC

Table 1, An overview of the changes in instrument.

After installation of the new detectors, a so-called telecover test [6] was carried out to inspect the overall optical alignment of the system. The results in Figure 3 show that overlap functions of the on and off wavelength are fairly similar, but only a perfect match allows artifact free DIAL measurements. The test points out that full overlap starts between 1.5 km and 2 km, which could theoretically be improved for our set-up. However, the installation of an additional small aperture near range telescope is planned to measure in ozone in the boundary layer.

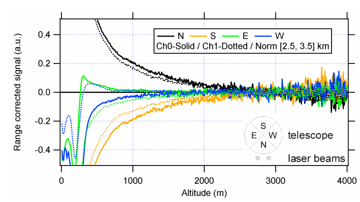

Figure 3, Telecover test carried out on June 2nd 2009. Full overlap between 1.5 km and 2 km.

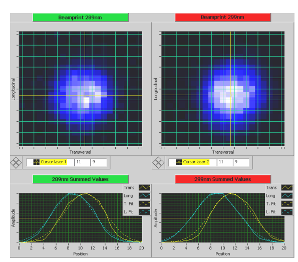

Figure 4, Partial screenshot of alignment program. A cross section of the laser beams at 2.25 km altitude is shown. Gaussian fits indicate optimal overlap positions.

3.2 Control software revision

The setup is operated from an industrial PC by a LabView program. A routine for repeatable, automated alignment of the laser beams was developed. After completion of the alignment scan, Gaussian fits of the beam profiles are created along their x and y axes.

The lasers are then positioned in the centres of these fits (Figure 4.).

3.3 Data processing software

Dataprocessing and visualisation routines are implemented in IgorPro.

3.3.1 Correction for systematic errors

The 10 nm wavelength separation introduces several systematic errors, related to differential extinction, backscatter and absorption. These errors can not be neglected and require correction [7].

Differential Rayleigh extinction can be corrected for using an atmospheric model (e.g. [8]) or radio sonde data. This error is largest at low altitudes and decreases with atmospheric density. The calculated correction decreases from 14,7 µg/m^3 at 1 km altitude to 5,7 µg/m^3 at 10 km.

3.3.2 Correction for aerosols

The presence of aerosols in the atmosphere produces two kinds of systematic errors. The first is related to differential extinction by aerosols and the second is caused by differential backscatter in regions with inhomogeneous aerosol concentrations. Errors of the second type are most prominently present at the top of the boundary layer.

$$n(R) = -\frac{1}{\Delta\sigma}\left\{\Delta\alpha_{abs}(R) + \Delta\alpha_{ext}(R)\right\}$$
$$\frac{1}{2\Delta\sigma}\frac{\delta}{\delta R}\left\{-\ln\left[\frac{P_{on}(R)}{P_{off}(R)}\right] + \ln\left[\frac{\beta_{on}(R)}{\beta_{off}(R)}\right]\right\}, \quad (1)$$

According to the DIAL equation (1), the ozone profile contains the sum of the extinction and backscatter effects. Therefore, a correction for both effects requires profiles of aerosol backscatter and extinction. Because these cannot be independently distilled from the measurement data, correcting for aerosol-related errors is not straightforward.

A method to correct for the error introduced by the presence of aerosols is suggested by Browell et al. [7]. This method is based on creating an aerosol backscatter and extinction profile from the offline return signal using assumptions about the aerosol properties. Based on this work, a correction for the error introduced by the presence of aerosols is being implemented. This method, however, still requires a priory information on the lidar ratio.

To improve this, preparations are made to install two additional channels for N_2 and O_2 Raman signals. These channels can be used to independently measure the aerosol profiles required for the corrections mentioned above. In addition, they can be used to perform DIAL on the Raman signals.

3.3.3 Cloud clearing

Because measurements cannot be used with cloud contamination, a routine was developed to detect clouds in measurement data and ignore any bursts containing clouds in further processing. Under cloudy conditions measurements can thus be carried out as usual.

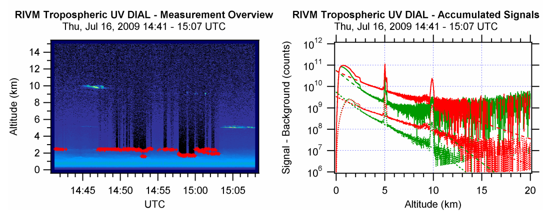

Figure 5, Left: An example of automated detection of clouds. Right: After filtering low-level clouds. Analog and photon counting data are shown with Rayleigh fits (dashed).

The routine is based on the detection of sharp peaks in the backscatter signal, to be attributed to clouds. The derivative of the backscatter signal exceeding a user-controlled threshold, removes bursts containing clouds form the signal average, as shown in Figure 5. The operator also controls the minimum and maximum detection altitudes. This can eliminate effects caused by the top of the boundary layer and clouds beyond the range of interest.

3.4 Measurement consistency and validation

The consistency of the measurement data can be checked in several ways: internally, using a modelled backscatter signal and externally, using balloon sonde data.

The modelled Rayleigh backscatter signal is based on radio sonde data from KNMI, or a modelled atmosphere [8]. To this atmospheric data, a simple, user-controlled ozone profile is added. These modelled signals are used to verify signal linearity.

The measurement data can be compared to external data from ozone sondes. Weekly routine launches of these sondes take place at KMI (Ukkel, B) and KNMI (De Bilt, NL). The KNMI launch site is conveniently located at only 2.6 km from the Tropospheric Ozone Lidar, the distance to Ukkel is 160 km.

4. COMPARING RECENT TO HISTORIC DATA

Between 1993 and 2003, routine measurements were performed. An example dataset with from this period is compared to a recent one. Both measurements include relevant balloon sonde data.

The older dataset is created on the 25th of July 1995. For this dataset, three profile segments are combined, covering the near, mid and far regime. The total combined measurement time was 1 hour. The recent dataset is created on the 16th of June 2009. In this dataset, a near and a far measurement with a total measurement time of 45 minutes are combined. The near measurement has a 10% data loss due to clouds. The data is processed with equal integration intervals for all measurements, so that the statistical integration noise, also called confidence margins, can be compared. The integration length increases quadratically, from 330 m at ground level to 1.5 km at 12 km. Both measurements are shown in Figure 6.

From the graphs, it can be seen that in both cases, sonde and lidar measurements match well above the lidar overlap range of 1-2km. The 2009 measurement shows deviations from the O_3 sonde between 8 and 10 km, which are most likely caused by atmospheric variations. This and other similar examples show that the system modifications have systematically increased the maximum measurement range into the lower stratosphere. However, in the near regime, the historic data shows a smaller confidence interval. The cause of this is currently not well understood, but might be due to imperfections in the optical alignment of the receiver.

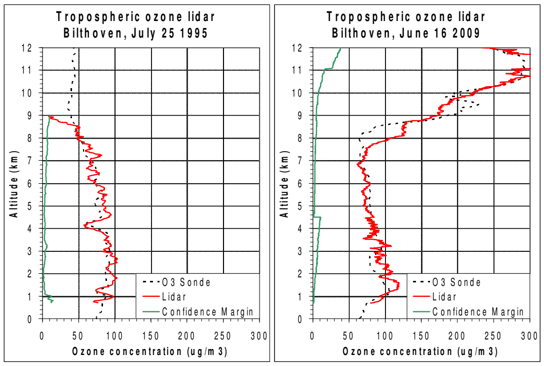

Figure 6, On the left the dataset from 1995, on the right the 2009 dataset. The 1995 dataset contains 18k/9k/9k shots in the near/mid/far regime. The sonde was launched at KNMI. The 2009 dataset contains 30k/45k shots in the near/far regime. The sonde was launched at KNMI at 12:51 UTC. Note the increased measurement range and the larger deviation in the near field of the 2009 measurement.

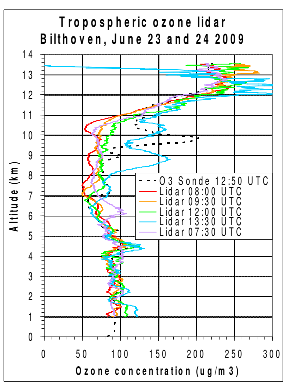

Figure 7, Intrusion forming on the 23rd and 24th of June 2009. The first four curves present data from the first day, the last curve (purple) shows data from the second day.

5. CINDI CAMPAIGN DATA

During the CINDI campaign in June and July of 2009, (http://www.knmi.nl/samenw/cindi/) the instrument was operated on 18 days, and on 5 of these days an ozone sonde was launched from the measurement site in Cabauw. The measurement data corresponds well to the sonde data and the dataset will be used in further validation studies of satellite data in the remainder of our project.

An ozone intrusion event happened on June 23rd and 24th. Figure 7 displays multiple measurements taken on these days and the data from the ozone sonde launched on the 23rd. The measurements show the variability in ozone concentrations over a time span of approximately 24 hours. It can be seen that on the 23rd the intrusion is formed and that during the night it has descended to lower altitudes. Note that the correlation between measurements and ozone sonde is very good up to 12 or even 13 km.

6. CONCLUSIONS

The tropO3 system has been improved and the measurement range now systematically reaches the lower stratosphere. However, the lower range (boundary layer) still requires further optimisation.

Participation in the CINDI campaign proved successful routine operation of the instrument. Multiple measurements per day show the capability to measure variability in ozone concentrations during the day, making the instrument ideally suited for studies of spatial and temporal variations and representativity.

The agreement between measurements and sonde data is very good, and multiple profiles can be acquired sequentially, confirming that the system is ready to be used for validation of satellite data.

Acknowledgement

Part of this work was funded by Netherlands Institute for Space Research (SRON)

REFERENCES

[1] Sunesson, J.A., Apituley, A., Swart, D.P.J., 1994: Differential absorption lidar system for routine monitoring of tropospheric ozone, *Appl. Opt.* **33** Issue 30, pp. 7045-7058

[2] Swart, D.P.J., Apituley, A., Spakman, J., Visser, E.P., Bergwerff, H.B., 1994: RIVMs tropospheric and stratospheric ozone lidars for european and global monitoring networks, *Proc. of the 17th ILRC*, pp. 405-408

[3] Apituley, A., Visser, E.P., Bergwerff, J.B., De Winter, J.M., De Backer, H., Alaart, M.A.F., 1996: RIVM tropospheric ozone LIDAR routine measurements validation and analyses, *Advances in Atmospheric Remote Sensing with LIDAR*, pp. 375-378

[4] Apituley, A., Visser, E.P., Bergwerf, J.B., de Winter, J.M., de Backer, H., Allaart, M.A.F., 1997: RIVM tropospheric ozone lidar routine measurements, validation, and analyses, *Advances in Atmospheric Remote Sensing*, pp. 375-378

[5] De Backer, H., Visser, E.P., De Muer, D., Swart, D.P.J., 1994: Potential for meteorological bias in lidar ozone data sets resulting from the restricted frequency of measurement due to cloud cover, *J. of Geophysical Res.* **99 (D1)**, pp. 1395-1401

[6] Freudenthaler, V., 2008: The Telecover Test: A quality assurance tool for the optical part of a lidar system, *Proc. ILRC24*.

[7] Browell E.V., Ismail S., Shipley S.T., 1985: Ultraviolet DIAL measurements of O_3 profiles in regions of spatially inhomogeneous aerosols, *App. Opt.*, **24** no. 17, pp 2827-2836

[8] National Oceanic and Atmospheric Administration, National Aeronautics and Space Administration, United States Air Force, 1976, U.S. Standard Atmosphere, 1976, U.S. Government Printing Office: 1976 0-588-256.